Generation of electrostatic solitary waves in the plasma sheet boundary layer

G. S. Lakhina,[1] S. V. Singh,[1,2] A. P. Kakad,[1] and J. S. Pickett[3]

Received 28 March 2011; revised 22 June 2011; accepted 24 July 2011; published 19 October 2011.

[1] Generation of electrostatic solitary waves (ESWs) in the plasma sheet boundary layer in terms of electron-acoustic solitons and double layers is proposed. The plasma sheet boundary layer is treated as a multicomponent magnetized plasma consisting of background electrons, counter-streaming electron beams and ions. The model is based on the multifluid equations and the Poisson equation, and uses the Sagdeev pseudo-potential technique. For the plasma parameters at the time of broadband electrostatic noise in the plasma sheet boundary layer observed by Cluster on 22 September 2004, the model predicts solitons/double layer with electric field ~(0.01–30) mV/m with time durations ~(0.1–4.5) ms. Such short electric field pulses, when Fourier transformed to the frequency domain, can appear as broadband electrostatic noise in the frequency range of ~220 Hz to 10 kHz. It is proposed that the model can be a good candidate for explaining the generation of broadband electrostatic noise in the plasma sheet boundary layer.

Citation: Lakhina, G. S., S. V. Singh, A. P. Kakad, and J. S. Pickett (2011), Generation of electrostatic solitary waves in the plasma sheet boundary layer, *J. Geophys. Res.*, *116*, A10218, doi:10.1029/2011JA016700.

1. Introduction

[2] From the analysis of the high time resolution of the plasma wave data from GEOTAIL, *Matsumoto et al.* [1994] showed for the first time that the broadband electrostatic noise (BEN) in the plasma sheet boundary layer (PSBL) actually consists of short electrostatic solitary waves (ESWs) whose Fourier spectrum gives rise to the broadband nature of the noise. Later on, ESWs have been observed at the bow shock [*Bale et al.*, 1998], in the magnetosheath [*Pickett et al.*, 2003, 2005], the polar cusp and polar cap boundary layer [*Franz et al.*, 1998; *Tsurutani et al.*, 1998; *Cattell et al.*, 1999], and on the auroral field lines [*Temerin et al.*, 1982; *Bostrom et al.*, 1988; *Mozer et al.*, 1997; *Ergun et al.*, 1998a, 1998b; *Bounds et al.*, 1999]. The ESWs are observed in the electric field component parallel to the background magnetic field, are usually bipolar, sometimes monopolar or tripolar, and are generally associated with electron or/and ion beams [*Omura et al.*, 1994; *Bounds et al.*, 1999]. The electrostatic solitary structures can have either positive or negative potentials, and their electric field amplitude can vary from a fraction of a mV/m in the plasma sheet boundary layer to several 100 mV/m in the dayside auroral zone [*Pickett et al.*, 2004; *Franz et al.*, 2005; *Ergun et al.*, 1998a, 1998b]. The velocities of ESWs can vary from ~ a few hundred to a few tens of thousand km s^{-1}, and their parallel scale sizes from ~100 m to tens of kilometer, as one moves outwards from the auroral region to the plasma sheet boundary layer [*Cattell et al.*, 1999; *Omura et al.*, 1999]. The most common interpretations for the ESWs observed in the PSBL are based on the nonlinear evolution of a bump-on-tail instability/electron two stream instability [*Omura et al.*, 1996; *Kojima et al.*, 1997; *Goldman et al.*, 1999; *Singh*, 2003] leading to the formation of Bernstein-Greene-Kruskal (BGK) [*Bernstein et al.*, 1957] potential structures (i.e., phase space electron holes) which reproduce well the observed electrostatic solitary waveforms.

[3] We would like to point out that the ESWs observed by spacecraft are characterized by an amplitude-width relationship where the amplitude of the potential, ϕ, of the solitary wave tends to increase with its width, W. This property of ESWs is opposite to that of KdV type solitons where the soliton amplitude increases as its width decreases. This shows that the ESWs observed by spacecraft are not the usual KdV type of small-amplitude ion-acoustic or electron-acoustic solitons. Actually, because of the misconception that all weak solitons would behave like KdV solitons, the generation mechanisms based on ion-acoustic or electron-acoustic solitons were considered unfeasible [*Ergun et al.*, 1998b; *Pickett et al.*, 2004; *Franz et al.*, 2005]. The properties of the arbitrary amplitude solitons predicted by the models based on the Sagdeev pseudo-potential techniques are different from the KdV type solitons; that is, depending upon the parametric range, their amplitudes can either increase or decrease with the increase of their width [*Ghosh and Lakhina*, 2004]. Therefore, the models based on arbitrary amplitude electron-acoustic solitary waves are promising in providing an alternate interpretation for the generation of ESWs [*Kakad et al.*, 2007; *Lakhina et al.*, 2008, 2009;

[1]Indian Institute of Geomagnetism, Navi Mumbai, India.
[2]School of Physics, University of Kwazulu-Natal, Durban, South Africa.
[3]Department of Physics and Astronomy, University of Iowa, Iowa, USA.

0148-0227/11/2011JA016700

Table 1. Properties of Electron-Acoustic Solitons and Double Layers, Such as Soliton Velocity (V), Potential (ϕ), Electric Field (E), Soliton Width (W) and Pulse Duration (τ), for Various Values of the Core and Beam Electron Densities, and Beam Velocities for the Case of Equal Density Counterstreaming Electron Beams[a]

	V_B/C_i = 10.0					V_B/C_i = 20.0				
$\frac{N_c}{n_0}, \frac{N_B}{n_0}$	V (10^3 km s^{-1})	ϕ (volt)	E (mV m^{-3})	W (km)	τ (ms)	V (10^3 km s^{-1})	ϕ (V)	E (mV m^{-3})	W (km)	τ (ms)
0.7, 0.15	13.6–14.1	−0.4 − −61.7	0.01–29.9	35.0–1.47	2.6–0.1	17.4–17.5	−0.3 − −8.9 (DL)	0.01–2.8	19.6–1.7	1.1–0.1
0.6, 0.20	14.5–14.6	−0.9 − −43.8 (DL)	0.02–4.2	40.5–9.9	2.8–0.7	17.8–17.9	0.4–36 (DL)	0.03–5.7	9.7–10.8	0.8–0.5
0.5, 0.25	15.5–15.6	0.8–127.9 (DL)	0.02–10.8	34.8–19.4	2.6–1.2	18.1–18.6	0.2–67.9	0.02–28.4	8.1–3.7	0.5–0.2
0.3, 0.35	17.1–18.2	0.4–108.8	0.02–41.9	18.0–3.3	1.1–0.2	18.6–19.1	0.1–11.6	0.01–10.2	6.2–1.5	0.3–0.1
0.1, 0.45	18.6–19.1	0.2–9.8	0.02–5.4	8.9–2.2	0.5–0.1	19.0–19.2	0.03–0.8	0.01–0.9	3.1–1.1	0.2–0.1

[a]The plasma sheet boundary layer parameters are taken as $n_0 = 0.3$ cm^{-3}, $T_i = 4$ keV, $T_c/T_i = 0.175$, $T_B/T_i = 0.005$. The double layers can occur at the maximum value of the velocity, V, and are marked as "DL" under the potential, ϕ.

Ghosh et al., 2008]. The earlier models of electron-acoustic solitons considered two/three temperature electron plasmas, and they could explain the space observations (e.g., Viking) of solitary waves which had negative potentials [*Pottelette et al.*, 1990; *Dubouloz et al.*, 1991, 1993; *S. V. Singh et al.*, 2001; *Singh and Lakhina*, 2004; *Tagare et al.*, 2004]. *Berthomier et al.* [2000] introduced an electron beam in the system having cold and hot electrons and they could obtain the positive potential structures. *Cattaert et al.* [2005] and *Verheest et al.* [2005] have shown that in two-electron-temperature plasmas, the electron-acoustic solitons having positive potentials can exist in some parametric range, even without the electron-beam component, provided the hot electron inertia is retained in the analysis.

[4] Recently, the plasma measurements made on the Cluster spacecraft in the plasma sheet boundary layer have shown that broadband (~2–6 kHz) electrostatic noise is associated with cold countersteaming electron beams flowing through the hot Maxwellian plasma [*Teste and Parks*, 2009]. The observed plasma parameters were (compare Table 1, under R1, of *Teste and Parks* [2009]): total electron density, n_0 = (0.27–0.32) cm^{-3}, core electron temperature, T_c = 600–800 eV, ion temperature, T_i = 3.7–5.0 keV, electron beams drift speed, v_B = 7000–12000 km s^{-1}, electron beams temperature, T_B = 10–100 eV, and magnetic field, B_0 = 8–12 nT. It is interesting to note these parameters are quite different than those employed in most theories for the PSBL ESWs based on two-stream instabilities with a bump-in-tail configuration, where the beam is hot and the back-ground electron population is cold [*Matsumoto et al.*, 1994]. *Teste and Parks* [2009] suggested that electrostatic waves could be produced by the nonlinear evolution of the electron-acoustic and electron-ion instability driven by the electron beams as discussed by *Schriver and Ashour-Abdalla* [1989]. We feel the theory of *Schriver and Ashour-Abdalla* [1989] cannot be applied directly to the present situation. First, their simulations of the electron-acoustic and electron-ion instabilities are done for a specific case where hot electron temperature and the ion temperature are the same, i.e., $T_c = T_i = 500\ T_B$ (in their notation $T_h = T_i = 500\ T_c$) which is not the case in the present situation. Second, their simulations are done for the ion-electron mass ratio, $m_i/m_e = 400$. It is not clear whether the instabilities will saturate at higher or lower level or at speeds faster or slower for the case of realistic mass ratio of 1836. Third, even when taking their results at the face value, the instabilities will destroy the electron beams in about $t = 100\omega_{pe}^{-1}$ (ω_{pe} being the electron plasma frequency) [*Schriver and Ashour-Abdalla*, 1989], i.e., in time less than 10 ms or so.

[5] Here, we propose an alternative generation mechanism for the PSBL electrostatic noise reported by *Teste and Parks* [2009] in terms of an electron-acoustic soliton model developed for the magnetosheath ESWs [*Lakhina et al.*, 2009]. This model deals with the time stationary state of the plasma system when the plasma instabilities, if present initially, have been saturated. In a sense, the model deals with the nonlinear modes of the system. We will adopt this model to the case of PSBL plasma parameters.

2. Electron-Acoustic Soliton/Double Layer Model

[6] We model the plasma sheet boundary layer plasma by a homogeneous, collisionless, and magnetized four component plasma consisting of hot core electrons (N_c, T_c, v_c), two cold electron beams (N_1, T_1, v_1) and (N_2, T_2, v_2) propagating along the magnetic field, and hot ions (N_i, T_i v_i), where N_j, T_j, v_j represent the equilibrium values of the density, temperature and beam velocity (along the direction of the ambient magnetic field) of the species j, and $j = i$, c, 1, and 2 for the ions, core electrons, beam 1 electrons and beam 2 electrons, respectively.

[7] For the nonlinear electrostatic waves propagating parallel to the magnetic field, the dynamics of the species is governed by the multifluid equations of continuity, momentum, and equation of state of each species, and the Poisson equation [*Lakhina et al.*, 2009, 2011] as

$$\frac{\partial n_j}{\partial t} + \frac{\partial (n_j v_j)}{\partial x} = 0 \tag{1}$$

$$\frac{\partial v_j}{\partial t} + v_j \frac{\partial v_j}{\partial x} + \frac{1}{\mu_j n_j} \frac{\partial P_j}{\partial x} - \frac{Z_j}{\mu_j} \frac{\partial \phi}{\partial x} = 0 \tag{2}$$

$$\frac{\partial P_j}{\partial t} + v_j \frac{\partial P_j}{\partial x} + 3P_j \frac{\partial v_j}{\partial x} = 0 \tag{3}$$

$$\frac{\partial^2 \phi}{\partial x^2} = n_c + n_1 + n_2 - n_i \tag{4}$$

where $\mu_j = m_j/m_i$, where m_j and m_i represent the mass of the jth species and the ions, respectively, and $Z_j = +1$ (−1) for electrons (ions), respectively. In equations (1)–(4), all densities are normalized with the unperturbed ion density, $N_i = N_c + N_1 + N_2$, velocities with the ion thermal velocity $C_i = (T_i/m_i)^{1/2}$, time with the inverse of ion plasma frequency,

$\omega_{pi} = (4\pi N_i e^2/m_i)^{1/2}$, the lengths with the ion Debye length, $\lambda_{di} = (T_i/4\pi N_i e^2)^{1/2}$, the electrostatic potential ϕ by T_i/e, and the thermal pressures P_j with $N_i T_i$. We have considered the same adiabatic index, i.e., $\gamma = 3$, for all the species in the equation of state (i.e., equation (3)). Here, we have normalized all the parameters with respect to ions as they are the hottest species in the PSBL. In principle, one can choose the normalization with respect to any of the electron species also.

[8] In order to study the properties of arbitrary amplitude electrostatic solitary waves, we transform the above set of equations to a stationary frame moving with velocity V, the solitary wave velocity, i.e., $\xi = (x - Mt)$ where $M = V/C_i$ is the Mach number with respect to the ion thermal velocity. Then, solving for perturbed densities, putting these expressions in the Poisson equation, and assuming appropriate boundary conditions for the localized disturbances along with the conditions that $\phi = 0$, and $d\phi/d\xi = 0$ at $\xi \rightarrow \pm\infty$, we get the following energy integral [*Lakhina et al.*, 2009, 2011],

$$\frac{1}{2}\left(\frac{\partial\phi}{\partial\xi}\right)^2 + \psi(\phi, M) = 0 \tag{5}$$

where the pseudopotential, $\psi(\phi, M)$, is known as the Sagdeev potential, and is given by,

$$\begin{aligned}
\psi(\phi, M) = {} & \mu n_c^0\left\{(M - v_c)^2 - \frac{(M - v_c)}{\sqrt{2}}B_c^{1/2}\right\} \\
& + n_c^0 T_c\left\{1 - 2\sqrt{2}(M - v_c)^3 B_c^{-3/2}\right\} \\
& + \mu n_1^0\left\{(M - v_1)^2 - \frac{(M - v_1)}{\sqrt{2}}B_1^{1/2}\right\} \\
& + n_1^0 T_1\left\{1 - 2\sqrt{2}(M - v_1)^3 B_1^{-3/2}\right\} \\
& + \mu n_2^0\left\{(M - v_2)^2 - \frac{(M - v_2)}{\sqrt{2}}B_2^{1/2}\right\} \\
& + n_2^0 T_2\left\{1 - 2\sqrt{2}(M - v_2)^3 B_2^{-3/2}\right\} \\
& + n_i^0\left\{(M - v_i)^2 - \frac{(M - v_i)}{\sqrt{2}}B_i^{1/2}\right\} \\
& + n_i^0\left\{1 - 2\sqrt{2}(M - v_i)^3 B_i^{-3/2}\right\}
\end{aligned} \tag{6}$$

Here,

$$\begin{aligned}
B_c &= A_c \pm \sqrt{A_c^2 - \frac{12T_c(M - v_c)^2}{\mu}} \\
B_1 &= A_1 \pm \sqrt{A_1^2 - \frac{12T_1(M - v_1)^2}{\mu}} \\
B_2 &= A_2 \pm \sqrt{A_2^2 - \frac{12T_2(M - v_2)^2}{\mu}} \\
B_i &= A_i \pm \sqrt{A_i^2 - 12(M - v_i)^2} \\
A_c &= (M - v_c)^2 + \frac{3T_c}{\mu} + \frac{2\phi}{\mu} \quad A_1 = (M - v_1)^2 + \frac{3T_1}{\mu} + \frac{2\phi}{\mu}, \\
A_2 &= (M - v_2)^2 + \frac{3T_2}{\mu} + \frac{2\phi}{\mu} \quad A_i = (M - v_i)^2 + 3 - 2\phi, \quad \mu = \frac{m_e}{m_i}
\end{aligned} \tag{7}$$

In equation (6), $n_j^0 = N_j/N_i$ such that $n_c^0 + n_1^0 + n_2^0 = n_i^0 = 1$, and the temperatures of the species are normalized with the ion temperature. We must point out that various B_js appearing in equation (7) are proportional to the square of the density of the respective jth species. Therefore, in order that various B_js are real, and the associated densities attain their undisturbed values in the limit of $\phi \rightarrow 0$ when $\xi \rightarrow \pm\infty$, we must use the + (plus) sign when the condition $(M - v_j)^2 + \frac{2\phi}{\mu} > \frac{3T_j}{\mu}$ is satisfied, and the minus sign when $(M - v_j)^2 + \frac{2\phi}{\mu} < \frac{3T_j}{\mu}$ holds [*Verheest et al.*, 2008; *Lakhina et al.*, 2009, 2011].

3. Soliton and Double Layer Solutions

[9] Equation (5) describes the motion of a pseudo-particle of unit mass in a pseudo-potential ψ where ϕ and ξ play the role of displacement x from the equilibrium and time t, respectively. It will give a soliton solution when the pseudo-particle is reflected in the pseudo-potential field and returns to its initial state (zero potential drop). Therefore, for soliton solutions, the Sagdeev potential $\psi(\phi, M)$ must satisfy the following conditions: $\psi(\phi, M) = 0$, $d\psi(\phi, M)/d\phi = 0$, $d^2\psi(\phi, M)/d\phi^2 < 0$ at $\phi = 0$, $\psi(\phi, M) = 0$ at $\phi = \phi_0$, and $\psi(\phi, M) < 0$ for $0 < |\phi| < |\phi_0|$. The double layer solutions could also exist at the upper limit on the Mach number $M = M_{DL}$ provided one more additional condition, namely, $d\psi(\phi, M)/d\phi = 0$ at $\phi = \phi_{DL}$ and $M = M_{DL}$, is satisfied. In such a case, the pseudo-particle is not reflected at $\phi = \phi_{DL}$ because of the vanishing pseudo-force and pseudo-velocities. Instead, it goes to another state producing an asymmetrical double layer (DL) with a net potential drop of ϕ_{DL}, where ϕ_{DL} is the amplitude of the double layer.

[10] From equation (6), it is seen that $\psi(\phi, M)$ and its first derivative with respect to ϕ vanish at $\phi = 0$. The condition $d^2\psi(\phi, M)/d\phi^2 < 0$ at $\phi = 0$ is satisfied provided $M > M_0$, where M_0 satisfies the equation

$$\begin{aligned}
f(M_0) \equiv {} & \frac{n_c^0}{\mu\left[(M_0 - v_c)^2 - \frac{3T_c}{\mu}\right]} + \frac{n_1^0}{\mu\left[(M_0 - v_1)^2 - \frac{3T_1}{\mu}\right]} \\
& + \frac{n_2^0}{\mu\left[(M_0 - v_2)^2 - \frac{3T_2}{\mu}\right]} + \frac{n_i^0}{\left[(M_0 - v_i)^2 - 3\right]} = 0
\end{aligned} \tag{8}$$

Equation (8) yields 6 roots but all the roots will not be physical. We will consider here only the real positive roots for M_0, or the critical Mach numbers representing the minimum admissible Mach number for the solitary solutions. Numerical solution of equation (8), in general yields three critical positive Mach numbers corresponding to an ion-acoustic and two (slow and fast) electron-acoustic beam modes. However, for a given set of plasma parameters, any one, two or all three of the modes can satisfy the soliton conditions given above.

4. Numerical Results

[11] We have numerically solved equation (6) for the Sagdeev potential, $\psi(\phi, M)$, as a function of ϕ for various values of Mach numbers $M > M_0$ for the case of counter-streaming electron beams having equal densities (i.e., $N_1 =$

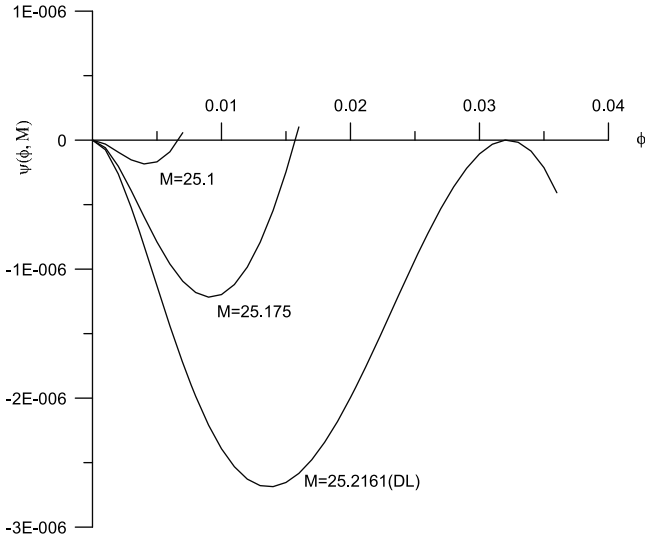

Figure 1. Variations of Sagdeev potential, $\psi(\phi, M)$, versus electrostatic potential, ϕ, for electron-acoustic solitons/double layer for the identical counterstreaming electron beams with plasma parameters: $v_c = v_i = 0.0$, $v_1 = -v_2 = v_B = 10.0$, $T_c = 0.175$, $T_B = 0.005$, $N_c/n_0 = 0.5$, $N_B/n_0 = 0.25$ and for $M = 25.10$, 25.175, and 25.2161.

$N_2 = N_B$) and temperature (i.e., $T_1 = T_2 = T_B$), and equal and opposite streaming velocities (i.e., $v_1 = -v_2 = v_B$). Based on the observations provided by *Teste and Parks* [2009], we consider the following normalized parameters for the numerical computations: $v_c = v_i = 0.0$, $T_c/T_i = 0.12$–0.22, $T_B/T_i = 0.002$–0.005, $v_B/C_i = 10.0$–20.0, and $N_c/n_0 = 0.1$–0.7 (correspondingly $N_B/n_0 = 0.45$–0.15). *Teste and Parks* [2009] do not give the relative number densities of the core electrons and beam electrons. Therefore, we have taken arbitrary values of the core and beam electron densities to cover the different cases where the total beam electron density ($2N_B$) is larger, equal and smaller as compared to the core electron density (N_c). For all these parameters we get only one critical Mach number M_0 corresponding to electron-acoustic solitons.

[12] Figure 1 shows the variation of Sagdeev potential $\psi(\phi, M)$ versus the normalized electrostatic potential ϕ for various values of the Mach number ($M > M_0$) for the case when the core electron density is equal to the density of both electron beams, i.e., $N_c = 2N_B$. The curves for $M = 25.10$ and 25.175 correspond to the electron-acoustic soliton solution, and the curve $M = 25.2161$ to the double layer solution. There are no soliton or double layer solutions for the Mach numbers exceeding 25.2161. It should be noted that the electron-acoustic solitons and double layer have positive potentials for the parameters considered here. This is essentially due to the retention of electron inertia effects in the analysis.

[13] Figure 2 shows the profiles of normalized electrostatic potential, ϕ obtained from the solution of equation (5), and corresponding to the parameters of Figure 1. It is interesting to note that the width (W) and amplitudes of ϕ tend to increase as Mach number, M increases.

[14] From Figures 1 and 2, it is clear that for the parameters of the PSBL, the electron-acoustic double layers having Mach number $M \sim 25$ are rather weak as $\phi \sim 0.03$ or so. Recently, *Sorasio et al.* [2006] have put forward a model of the very high Mach number electrostatic shocks resulting from the collision of plasma slabs with different temperatures and densities. The shock transition region is modeled as a planar one dimensional double layer. They predict large values of electrostatic potential $\phi_S = e\phi/T_{eL} \sim 10$–$200$ for shock wave Mach numbers $M_S = V/V_s \sim 10$–20 or higher [see *Sorasio et al.*, 2006, Figure 2]. Here T_{eL} is the cold electron temperature on the lower potential side of the double layer, and $V_s = T_{eL}/m_i$ is the ion acoustic speed. In our case, in the normalization of ϕ the ion temperature is used as opposed to the electron temperature. Even when ϕ is normalized with the beam electron temperature, we get $e\phi/T_B \sim 6$ which is much smaller than ϕ_S. The reason for this apparent contradictory result lies in the different approaches on which the two models are based and also the choice of plasma parameters. Our model is based on the multifluid approach, whereas the shock model of *Sorasio et al.* [2006] adopts a kinetic approach for the electrons (free and trapped electron populations) and treats ions as a fluid. Another important difference between their and our model concerns the limit on the amplitude of the double layer potential. *Sorasio et al.* [2006] take the upper limit on potential as $\phi_{cr} = M^2/2$ which corresponds to infinite compression of the cold ions by the shock electric field whereas in our case, the amplitude of the double layer, ϕ_{DL}, is decided by the charge neutrality condition, i.e., $d\psi(\phi, M)/d\phi = 0$ at $\phi = \phi_{DL}$. Further, the plasma parameters for the PSBL events are such that the ions are the hottest species, whereas in the model of *Sorasio et al.* [2006] the ions are treated as a cold fluid. Therefore, the results of the *Sorasio et al.* [2006] model cannot be applied to the present case.

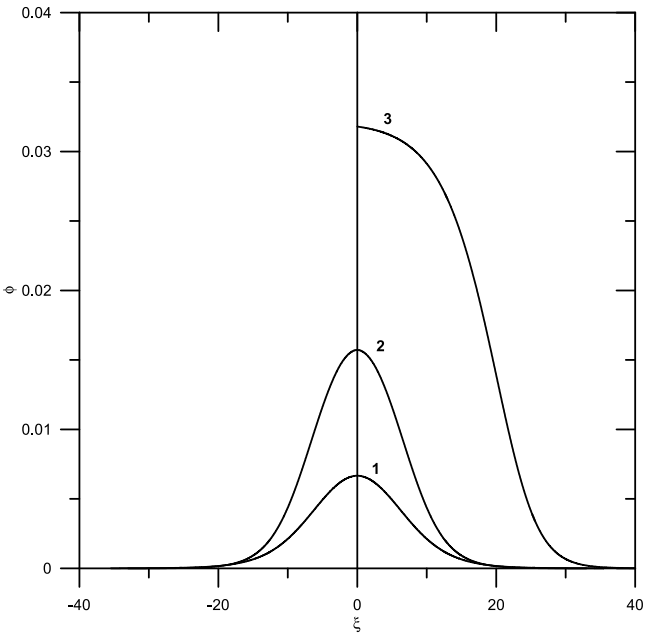

Figure 2. The profiles for electrostatic potential, ϕ for the electron-acoustic solitons/double layer for the parameters of Figure 1. Curves 1, 2 and 3 are for the Mach number $M = 25.10$, 25.175, and 25.2161, respectively. These can be taken as typical electrostatic potential profiles.

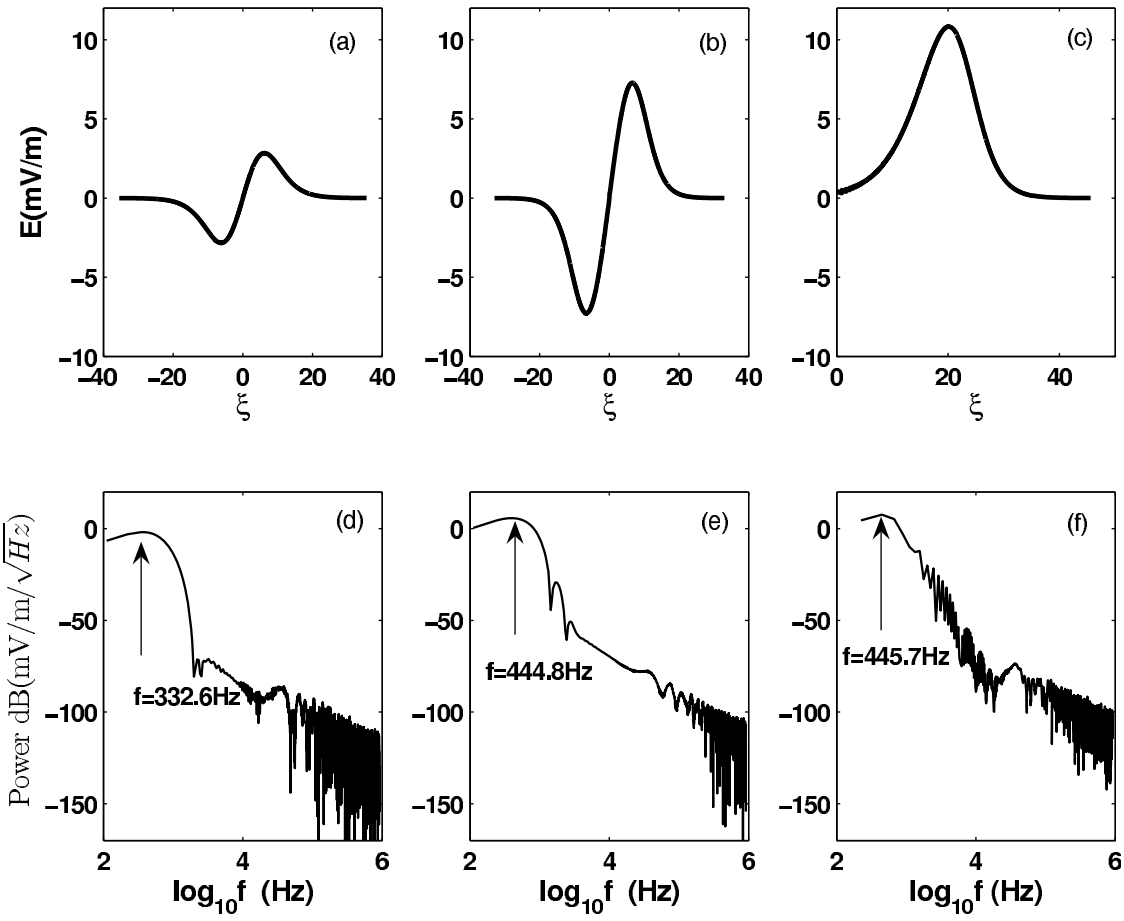

Figure 3. The profiles for electric field, E, versus the normalized spatial coordinate, ξ, for the electron-acoustic solitons/double layer corresponding to electrostatic potential, ϕ, profiles shown in Figure 2 for (a) $M = 25.10$, (b) 25.175, and (c) 25.2161. (d, e and f) The corresponding fast Fourier transform (FFT) power spectra of the electric fields shown in Figures 3a, 3b, and 3c. The x-axis represents the $\log_{10} f$, where f is the frequency in Hz. The y-axis denotes the power of the electric field expressed in units of dB (mV/m/$\sqrt{Hz}$).

[15] Figures 3a, 3b, and 3c show the profiles of the electric field E, corresponding to potential, ϕ, profiles shown in Figure 2. The electric field has a bipolar structure for the solitons (Figures 3a and 3b) and a monopolar structure for the double layer (Figure 3c). Figures 3d, 3e and 3f show the fast Fourier transform (FFT) power spectra of the electric fields shown in Figures 3a, 3b, and 3c, respectively. In all the three cases, the frequency, f, in the range of 330–450 Hz contributes maximum to the electric field structures. It is interesting to note that the first peak in power spectrum occurs near the inverse of the time duration of the soliton/double layer, $\tau = W/V$ (where W is the soliton width and V is the soliton velocity). The maximum electric field amplitudes are in the range of 4–12 mV/m. It should be noted that the power in the power spectrum decreases as frequency increases. The power spectrum tends to noise level for frequencies beyond 10–12 kHz.

[16] The properties of electron-acoustic solitons and double layers such as their velocities, V, electric potential, ϕ, magnitude of the electric field E, soliton/double layer width, W, and time duration, $\tau = W/V$, are given in Tables 1 and 2 for the parameters observed in the PSBL. For each case, the electron-acoustic solitons can exist over a range of V, W, τ, ϕ and E. However, the double layers have only one value of these parameters (the highest value of the range under each column). For example, the double layer velocity is simply the highest value of V mentioned in Tables 1 and 2. Further, the double layers, if they exist, are indicated by "DL" under the potential ϕ in Table 1. In Table 2, the ϕ values are not shown as the solitary structures have positive potentials which end up with double layers for all the cases.

[17] From Table 1, it is clear that for a relative core electron density smaller than 0.6 the solitons and double layers have positive potentials whereas for $N_c/n_0 \geq 0.6$, they may have negative potentials (see first two sets of ϕ values in Table 1). An increase in beam velocity shifts the soliton velocity to higher values but leads to a reduction in the values of ϕ, E, W and pulse duration as well as their ranges. *Cattaert et al.* [2005] have given an explanation for the transition from negative to positive potential solitons/double layer in terms of the cold electron density increasing from a small to a large value in the gasdynamics formalism involving the sonic points of cold and hot electrons and the charge neutral points. According to them, at small values of

Table 2. Variations of Soliton Velocity (V), Electric Field (E), Soliton Width (W) and Pulse Duration (τ), for Various Values of the Core and Beam Electron Temperatures for the Parameters of Table 1 Except That $N_c/n_0 = 0.5$, $N_B/n_0 = 0.25$, $V_B/C_i = 10.0$[a]

	$T_b/T_i = 0.002$				$T_b/T_i = 0.005$			
T_c/T_i	V (10^3 km s^{-1})	E (mV m^{-1})	W (km)	τ (ms)	V (10^3 km s^{-1})	E (mV m^{-1})	W (km)	τ (ms)
0.125	13.4–13.6	0.01–12.6	38.2–12.5	2.9–0.9	13.6–13.7	0.004–9.8	45.2–11.6	3.3–0.8
0.150	14.4–14.6	0.01–12.6	39.0–12.8	2.7–0.9	14.6–14.7	0.01–10.3	46.8–14.3	3.2–1.0
0.175	15.3–15.5	0.01–12.9	52.2–16.0	3.4–1.0	15.5–15.6	0.01–10.8	58.3–12.9	3.77–0.8
0.200	16.2–16.4	0.01–13.3	73.5–16.1	4.5–1.0	16.4–16.5	0.01–11.4	59.2–20.7	3.6–1.3
0.225	17.0–17.2	0.01–13.8	77.9–18.5	4.58–1.0	17.1–17.3	0.01–12.1	97.8–19.6	5.7–1.1

[a]Here, the potential ϕ is not shown since the solitons have positive potentials and the double layers occur for all the cases at the maximum value of the velocity, V.

cold electron (in our case beam electron) density, the cold electron sonic point is reached first, which compresses the cold electrons and produces negative potential solitary structures. When the cold electron density is increased above a certain value, the hot electron sonic point is reached first where the hot electrons are accelerated and rarefied producing positive potential solitary structures.

[18] Table 2 shows that increases in core electron and beam electron temperatures, in general, tend to increase the soliton and double layer velocities, electric field amplitude, soliton width and pulse duration.

5. Discussion

[19] Multispecies plasma, e.g., cold background (electron-ion) plasma and cold/hot electron-ion beams have been observed in the magnetosphere by several spacecraft. The cold plasma (temperatures a few eVs) originates in the ionosphere and the hot plasma (temperatures 100s eVs to a few keVs) comes from the magnetosphere. The intermixing of cold and hot plasmas occurs in the flow boundary, like, magnetopause, plasma sheet boundary layer, polar cusp and auroral field lines, etc. The multicomponent plasmas containing cold and hot electrons and ions, formed by the mixing of two plasmas of different temperatures, could exist on a timescale shorter than the thermalization time, which in the collisionless space plasmas could be very large, of the order of several hours to days in the magnetosphere. The timescales we are dealing with are very short, ~ milliseconds to seconds, and hence we are justified in treating the multispecies as multifluids.

[20] The theoretical model for the electrostatic solitary waves presented here is quite general and can be applied to other space and astrophysical plasma situations where multicomponent magnetized plasmas consisting of core electrons, counterstreaming electron beams and ions are present. The characteristics of the solitary waves and double layer will depend on the plasma parameters of the system. For example, the normalized amplitudes of the double layers for the magnetosheath plasma parameters are found to be ~0.02–0.15 [*Lakhina et al.*, 2009], whereas for the PSBL case, they are ~0.03–0.05. However, our model is valid for the parallel propagating ESWs which are not affected by the ambient magnetic field. The obliquely propagating electrostatic solitary waves are significantly affected by the magnetic field [see *Ghosh et al.*, 2008]. In fact, the electron magnetization plays an important role on the structure as well as stability of the ESWs. *Franz et al.* [2000] have shown that ESWs observed by the Polar spacecraft are roughly spherical for $R = f_{ce}/f_{pe} > 1$ (f_{ce} and f_{pe} being the electron cyclotron frequency and the electron plasma frequency, respectively), and become more oblate (with perpendicular scale larger than the parallel scale) as R decreases to less that 1. *N. Singh et al.* [2001] have carried out 3D particle simulations of electron holes (e-holes) and found that e-holes are essentially planar and highly transitory for $R < 1$, while for $R \geq 2$ they are long-lasting and can have a variety of structures from spherical to planar. During the interval of interest, the electron plasma frequency was $f_{pe} \approx$ (4.7–5.1) kHz and electron cyclotron frequency was $f_{ce} \approx$ (220–330) Hz in the PSBL [*Teste and Parks*, 2009], thus giving R = (0.04–0.07). Since $R \ll 1$, the long-lasting electron phase space holes are most unlikely to exist in the PSBL for the case considered here.

[21] The model presented here allows the existence of electron-acoustic solitons and double layers for the plasma sheet boundary layer parameters reported by *Teste and Parks* [2009]. The electric field amplitudes, parallel widths, velocities and time duration of the electron-acoustic solitons/double layers predicted by the models are in the range of ~(0.01–30) mV/m, ~(1–100) km, ~(13.4–19.2)10^3 km s^{-1}, and ~(0.1–4.5) ms, respectively (see Tables 1 and 2). These characteristics are in good agreement with the properties of ESWs in the plasma sheet boundary layer observed by the Geotail spacecraft [*Omura et al.*, 1999, Table 1]. The power spectrum analysis of the soliton/double layer electric field implies that a broadband range of frequencies from ~220 Hz to 10 kHz can be generated. The peak power lies at the frequency corresponding to τ^{-1}, i.e., the inverse of the soliton/double layer time duration.

[22] Unfortunately, the Cluster WBD waveform data for this event discussed by *Teste and Parks* [2009] are not available to confirm the presence of bipolar and monopolar pulses predicted by our analysis. However, we note that the pulse durations of ~(0.1–4.5) ms, typical for the PSBL as shown in Figures 3 and 4 of *Pickett et al.* [2004] from Cluster WBD measurements and as exemplified in a plasma sheet case study during a substorm onset [*Pickett et al.*, 2009], could give rise to broadband electrostatic emissions ranging from ~220 Hz to 10 kHz. This agrees well with the results of Figures 3d–3f. Further, the amplitude of the intense electrostatic emissions (~0345–0346:50 UT on 22 September 2004 [see *Teste and Parks*, 2009, Figure 2]) is seen to be $\delta E \sim$ (0.05–0.1) mV/m. It is noticed that both the observed frequency range (~2–6 kHz) and electric field amplitude are within the limit of predicted values by the electron-acoustic soliton model. In fact, the predicted electric fields, corresponding to the lower range of soliton

velocity ranges in Tables 1 and 2, seem to be in excellent agreement with the observed δE. The predicted E amplitudes (~10–30 mV/m) of the solitary structures near the upper range of soliton velocities appear to be much higher than δE deduced from the spectrogram of the ES waves. In view of the fact that the observed spectrogram is produced over a time period of ~80 ms, whereas the pulse duration of the solitary waves near the upper range of soliton velocities are typically ~0.1–1.0 ms (see Tables 1 and 2), the discrepancy is expected. To summarize, the generation of broadband electrostatic noise observed in the plasma sheet boundary layer by *Teste and Parks* [2009] may be explained by the electron-acoustic soliton/double layer model discussed here.

[23] **Acknowledgments.** G.S.L. thanks the Indian National Science Academy, New Delhi, for the support under the Senior Scientist scheme. J.S.P. acknowledges support from NASA Goddard Space Flight Center under grant NNX11AB38G. Thanks are due to Bharati Kakad for help in producing Figure 3.

[24] Philippa Browning thanks the reviewers for their assistance in evaluating this paper.

References

Bale, S. D., P. J. Kellogg, D. E. Larson, R. P. Lin, K. Goetz, and R. P. Lepping (1998), Bipolar electrostatic structures in the shock transition region: Evidence of electron phase space holes, *Geophys. Res. Lett.*, *25*, 2929–2932.

Bernstein, I. B., J. M. Greene, and M. D. Kruskal (1957), Exact nonlinear plasma oscillations, *Phys. Rev.*, *108*, 546–550.

Berthomier, M., R. Pottelette, M. Malingre, and Y. Khotyaintsev (2000), Electron acoustic solitons in an electron-beam plasma system, *Phys. Plasmas*, *7*, 2987–2994.

Bostrom, R., G. Gustafsson, G. Holback, G. Holmgren, H. Koskinen, and P. Kintner (1988), Characteristics of solitary waves and weak double layers in the magnetospheric plasma, *Phys. Rev. Lett.*, *61*, 82–85.

Bounds, S. R., R. F. Pfaff, S. F. Knowlton, F. S. Mozer, M. A. Temerin, and C. A. Kletzing (1999), Solitary potential structures associated with ion and electron beams near 1 R_E altitude, *J. Geophys. Res.*, *104*, 28,709–28,717.

Cattaert, T., F. Verheest, and M. A. Hellberg (2005), Potential hill electron-acoustic solitons and double layers in plasmas with two electron species, *Phys. Plasmas*, *12*, 042901, doi:10.1063/1.1868733.

Cattell, C. A., et al. (1999), Comparisons of Polar satellite observations of solitary wave velocities in the plasma sheet boundary and the high altitude cusp to those in the auroral zone, *Geophys. Res. Lett.*, *26*, 425–428.

Dubouloz, N., R. Pottelette, M. Malingre, and R. A. Treumann (1991), Generation of broadband electrostatic noise by electron acoustic solitons, *Geophys. Res. Lett.*, *18*, 155–158.

Dubouloz, N., R. A. Treumann, R. Pottelette, and M. Malingre (1993), Turbulence generated by a gas of electron acoustic solitons, *J. Geophys. Res.*, *98*, 17,415–17,422.

Ergun, R. E., et al. (1998a), FAST satellite observations of large-amplitude solitary structures, *Geophys. Res. Lett.*, *25*, 2041–2044.

Ergun, R. E., C. W. Calrson, J. P. McFadden, F. S. Mozer, L. Muschietti, I. Roth, and R. J. Strangeway (1998b), Debye-scale plasma structures associated with magnetic-field-aligned electric fields, *Phys. Rev. Lett.*, *81*, 826–829.

Franz, J. R., P. M. Kintner, and J. S. Pickett (1998), POLAR observations of coherent electric field structures, *Geophys. Res. Lett.*, *25*, 1277–1280.

Franz, J. R., P. M. Kintner, C. E. Seyler, J. S. Pickett, and J. D. Scudder (2000), On the perpendicular scale of electron phase-space holes, *Geophys. Res. Lett.*, *27*, 169–172.

Franz, J. R., P. M. Kintner, J. S. Pickett, and L.-J. Chen (2005), Properties of small-amplitude electron phase-space holes observed by Polar, *J. Geophys. Res.*, *110*, A09212, doi:10.1029/2005JA011095.

Ghosh, S. S., and G. S. Lakhina (2004), Anomalous width variation of rarefactive ion acoustic solitary waves in the context of auroral plasmas, *Nonlinear Processes Geophys.*, *11*, 219–228.

Ghosh, S. S., J. S. Pickett, G. S. Lakhina, J. D. Winningham, B. Lavraud, and P. M. E. Decreau (2008), Parametric analysis of positive amplitude electron acoustic solitary waves in a magnetized plasma and its application to boundary layers, *J. Geophys. Res.*, *113*, A06218, doi:10.1029/2007JA012768.

Goldman, M. V., M. M. Oppenheim, and D. L. Newman (1999), Nonlinear Two-Stream Instabilities as an explanation for the auroral bipolar wave structures, *Geophys. Res. Lett.*, *26*, 1821–1824.

Kakad, A. P., S. V. Singh, R. V. Reddy, G. S. Lakhina, S. G. Tagare, and F. Verheest (2007), Generation mechanism for electron acoustic solitary waves, *Phys. Plasmas*, *14*, 052305, doi:10.1063/1.2732176.

Kojima, H., H. Matsumoto, S. Chikuba, S. Horiyama, M. Ashour-Abdalla, and R. R. Anderson (1997), Geotail waveform observations of broadband/narrowband electrostatic noise in the distant tail, *J. Geophys. Res.*, *102*, 14,439–14,455.

Lakhina, G. S., A. P. Kakad, S. V. Singh, and F. Verheest (2008), Ion-and electron-acoustic solitons in two-electron temperature space plasmas, *Phys. Plasmas*, *15*, 062903, doi:10.1063/1.2930469.

Lakhina, G. S., S. V. Singh, A. P. Kakad, M. L. Goldstein, A. F. Viñas, and J. S. Pickett (2009), A mechanism for electrostatic solitary structures in the Earth's magnetosheath, *J. Geophys. Res.*, *114*, A09212, doi:10.1029/2009JA014306.

Lakhina, G. S., S. V. Singh, and A. P. Kakad (2011), Ion- and electron-acoustic solitons and double layers in multi-component space plasmas, *J. Adv. Space Res.*, *47*, 1558–1567, doi:10.1016/j.asr.2010.12.013.

Matsumoto, H., H. Kojima, T. Miyatake, Y. Omura, Y. M. Okada, I. Nagano, and M. Tsutui (1994), Electrostatic solitary waves (ESW) in the Magnetotail: BEN wave forms observed by GEOTAIL, *Geophys. Res. Lett.*, *21*, 2915–2918.

Mozer, F. S., R. E. Ergun, M. Temerin, C. Cattell, J. Dombeck, and J. Wygant (1997), New features of time domain electric field structures in the auroral acceleration region, *Phys. Rev. Lett.*, *79*, 1281–1284.

Omura, Y., H. Kojima, and H. Matsumoto (1994), Computer simulation of electrostatic solitary waves: A nonlinear model of broadband electrostatic noise, *Geophys. Res. Lett.*, *21*, 2923–2926.

Omura, Y., H. Matsumoto, T. Miyake, and H. Kojima (1996), Electron beam instabilities as generation mechanism of electrostatic solitary waves in the magnetotail, *J. Geophys. Res.*, *101*, 2685–2697.

Omura, Y., H. Kojima, N. Miki, T. Mukai, H. Matsumoto, and R. Anderson (1999), Electrostatic solitary waves carried by diffused electron beams observed by the Geotail spacecraft, *J. Geophys. Res.*, *104*, 14,627–14,637.

Pickett, J. S., J. D. Menietti, D. A. Gurnett, B. T. Tsurutani, P. Kintner, E. Klatt, and A. Balogh (2003), Solitary potential structures observed in the magnetosheath by the Cluster spacecraft, *Nonlinear Processes Geophys.*, *10*, 3–11.

Pickett, J. S., L.-J. Chen, S. W. Kahler, O. Santolik, D. A. Gurnett, B. T. Tsurutani, and A. Balogh (2004), Isolated electrostatic structures observed throughout the Cluster orbit: Relationship to magnetic field strength, *Ann. Geophys.*, *22*, 2515–2523.

Pickett, J. S., et al. (2005), On the generation of solitary waves observed by Cluster in the near-Earth magnetosheath, *Nonlinear Processes Geophys.*, *12*, 181–193.

Pickett, J. S., et al. (2009), Electrostatic solitary waves in current layers: From Cluster observations during a super-substorm to beam experiments at the LAPD, *Nonlinear Processes Geophys.*, *16*, 431–442.

Pottelette, R., M. Malingre, N. Dubouloz, B. Aparicio, R. Lundin, G. Holmgren, and G. Marklund (1990), High frequency waves in the Cusp/cleft Regions, *J. Geophys. Res.*, *95*, 5957–5971.

Schriver, D., and M. Ashour-Abdalla (1989), Broadband electrostatic noise due to field-aligned currents, *Geophys. Res. Lett.*, *16*, 899–902.

Singh, N. (2003), Space-time evolution of electron-beam driven electron holes and their effects on the plasma, *Nonlinear Processes Geophys.*, *10*, 53–63.

Singh, N., S. M. Loo, and E. Wells (2001), Electron hole structure and its stability depending on plasma magnetization, *J. Geophys. Res.*, *106*, 21,183–21,198.

Singh, S. V., and G. S. Lakhina (2004), Electron acoustic solitary waves with non-thermal distribution of electrons., *Nonlinear Processes Geophys.*, *11*, 275–279.

Singh, S. V., R. V. Reddy, and G. S. Lakhina (2001), Broadband electrostatic noise due to nonlinear electron acoustic waves, *Adv. Space Res.*, *28*, 1643–1648.

Sorasio, G., M. Marti, R. Fonseca, and L. O. Silva (2006), Very high Mach-number electrostatic shocks in collisionless plasmas, *Phys. Rev. Lett.*, *96*, 045005, doi:10.1103/PhysRevLett.96.045005.

Tagare, S. G., S. V. Singh, R. V. Reddy, and G. S. Lakhina (2004), Electron acoustic solitons in the Earth's magnetotail, *Nonlinear Processes Geophys.*, *11*, 215–218.

Temerin, M., K. Cerny, W. Lotko, and F. S. Mozer (1982), Observations of double layers and solitary waves in the auroral plasma, *Phys. Rev. Lett.*, *48*, 1175–1179.

Teste, A., and G. K. Parks (2009), Counterstreaming beams and flat-top electron distributions observed with Langmuir, Whistler, and compressional Alfvén waves in Earth's magnetic tail, *Phys. Rev. Lett.*, *102*, 075003, doi:10.1103/PhysRevLett.102.075003.

Tsurutani, B. T., J. K. Arballo, G. S. Lakhina, C. M. Ho, B. Buti, J. S. Pickett, and D. A. Gurnett (1998), Plasma waves in the dayside polar cap boundary layer: Bipolar and monopolar electric pulses and whistler mode waves, *Geophys. Res. Lett.*, *25*, 4117–4120.

Verheest, F., T. Cattaert, and M. Hellberg (2005), Compressive and rarefactive electron-acoustic solitons and double layers in space plasmas, *Space Sci. Rev.*, *121*, 299–311.

Verheest, F., M. A. Hellberg, and I. Kourakis (2008), Acoustic solitary waves in dusty and/or multi-ion plasmas with cold, adiabatic, and hot constituents, *Phys. Plasmas*, *15*, 112309, doi:10.1063/1.3026716.

A. P. Kakad, G. S. Lakhina, and S. V. Singh, Indian Institute of Geomagnetism, Plot 5, Sector-18, New Panvel (W), Navi Mumbai 410 218, India. (amar@iigs.iigm.res.in; lakhina@iigs.iigm.res.in; satyavir@iigs.iigm.res.in)

J. S. Pickett, Department of Physics and Astronomy, University of Iowa, Office 715 Van Allen Hall, Iowa City, IA 52242, USA. (pickett@uiowa.edu)